

Supporting information for

Directionally-Controlled Periodic Collimated Beams of Surface Plasmon Polaritons on Metal Film in Ag Nanowire/Al₂O₃/Ag Film Composite Structure

Hong Wei,* Xiaorui Tian, Deng Pan, Li Chen, Zhili Jia, and Hongxing Xu*

Institute of Physics, Chinese Academy of Sciences, and Beijing National Laboratory
for Condensed Matter Physics, Beijing 100190, China

Corresponding Authors

*E-mail: (H.X.X.) hxxu@iphy.ac.cn

*E-mail: (H.W.) weihong@iphy.ac.cn

1. Sample preparation and optical measurements

After the glass substrates were cleaned by washing, silver film of 120 nm thickness was deposited on the glass substrates by electron-beam evaporation. Then a dielectric layer of Al₂O₃ was deposited using an atomic layer deposition system (Cambridge NanoTech, Savannah-100) at 200°C. Silver nanowires (NWs) dispersed in ethanol were then dropped onto the Al₂O₃ layer surface. Additional Al₂O₃ of 30 nm thickness was deposited on top. Finally, semiconductor quantum dots (Invitrogen, Catalog No. Q21321MP) were spin-coated onto the sample surface.

Optical measurements were performed using an Olympus BX 51 microscope. Laser light of 633 nm wavelength was directed to the microscope and focused onto the end of the NW through a 100× objective (NA 0.95). The signal was collected by the same objective and directed to a CCD camera (DVC-1412AM). A long-pass edge filter was used to block the excitation laser to record the fluorescence of quantum dots. The

central emission wavelength of the quantum dots is about 655 nm.

2. Quantum-dot-fluorescence image of the nanowire-on-film structure

To see clearly the periodic near-field distribution on the nanowire, the image in Figure 1d is shown here at a different intensity scale.

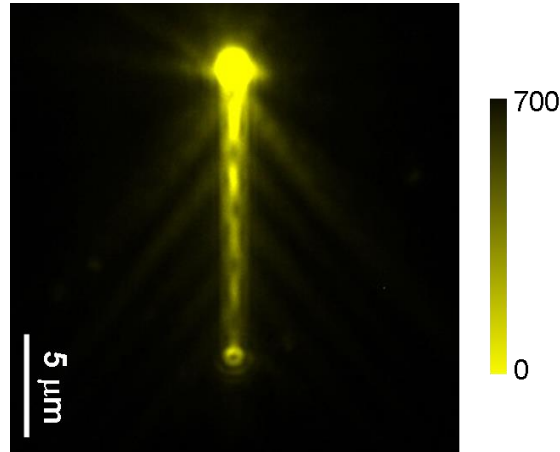


Figure S1. Quantum-dot-fluorescence image of the NW in Figure 1d shown at a different intensity scale.

3. Distribution of film SPPs for three modes on nanowire

When the polarization of the incident laser is at an angle with respect to the NW, three modes can be excited.^{1,2} For the Ag NW/Al₂O₃/Ag film composite structure in this study, besides the two SPP modes (MI and MII) generated by the laser polarized parallel to the NW, another mode (named MIII) can be excited when the polarization is perpendicular to the NW. Figure S2 shows the field distribution and the $\text{Re}(k)$ dependence on the spacer thickness H of the mode MIII. This mode is also a leaky mode, as its effective refractive index ($\text{Re}(k)/k_0$) is lower than that of the SPPs on the film.

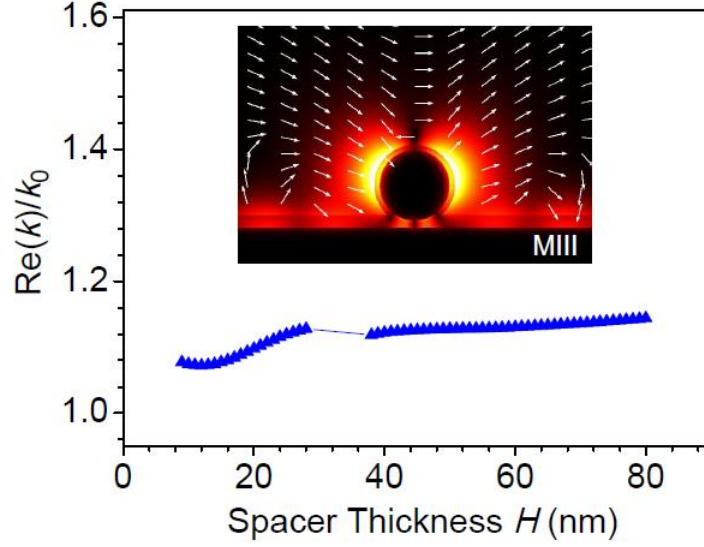


Figure S2. Simulated electric field distribution and real part of the wave vector $\text{Re}(k)$ of the additional SPP mode on the NW as a function of the spacer thickness H .

The SPP waves on the film excited by the three modes on the NW will lead to a more complex interference pattern. The interference pattern of the three SPP waves on

the film is expressed as:
$$I = \left| \sum_i A_i \exp[-ik_F (\cos \theta_i x + \sin \theta_i y)] \right|^2 \quad (i = \text{MI, MII, MIII}),$$

where k_F is the wave vector of SPPs on the film, A_i and θ_i are the amplitude and radiation angle of the SPP waves from corresponding mode on the NW. The radiation angle is calculated as in the main text using $\cos \theta_i = \text{Re}(k_i) / \text{Re}(k_F)$ ($i = \text{MI, MII, MIII}$), where k_i is the wave vector of the NW modes shown in Figure 3b and Figure S2. Here, we use equal amplitudes A_i and the values of k_i and k_F at $H = 50$ nm for the calculation. Figure S3 shows the calculation results for two SPP waves corresponding to modes MI and MII (Figure S3a), and for three SPP waves corresponding to modes MI, MII and MIII (Figure S3b). As can be seen, the additional mode will truncate the collimated beams periodically. In experiments, we also see the evidence of the excitation of mode MIII by the changed collimated beams shown in Figure S4. In experiments, the collimated film SPP beams formed by modes MI and MII are dominating, which may be due to the small amplitude of the electric field for mode MIII.

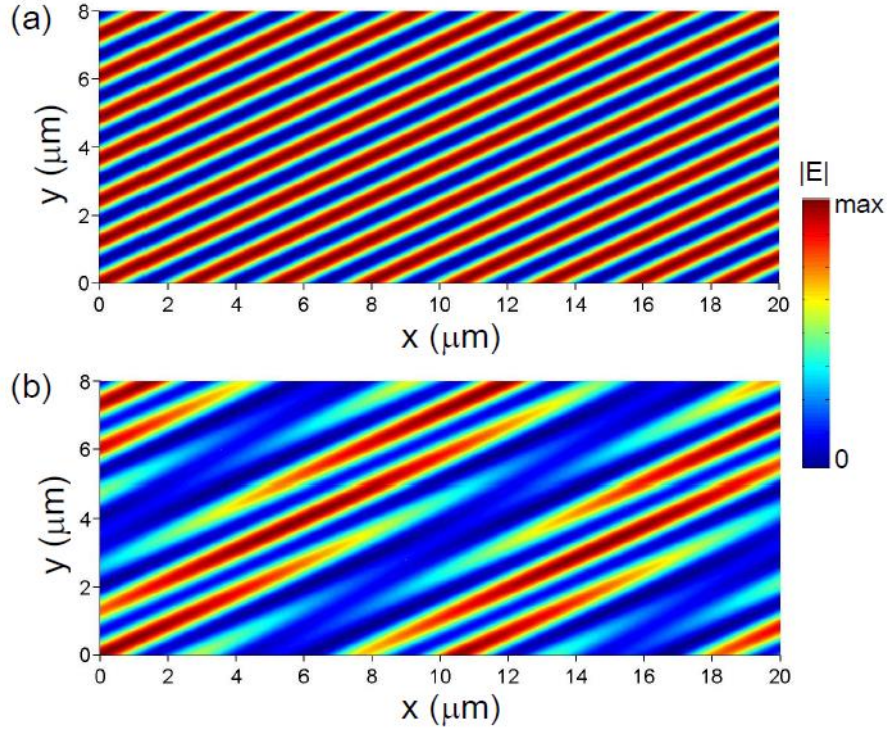


Figure S3. (a) Interference pattern of two plane waves corresponding to the two film-SPP waves generated by modes MI and MII on the NW. (b) Interference pattern of three plane waves corresponding to the three film-SPP waves generated by modes MI, MII and MIII on the NW. The directions of the plane waves with respect to the x direction correspond to the directions of the film-SPP waves with respect to the NW for $H = 50$ nm (obtained from Figure 3b and Figure S2). The value of the wave vector for the plane waves is set to the $\text{Re}(k)$ value of film SPPs for $H = 50$ nm.

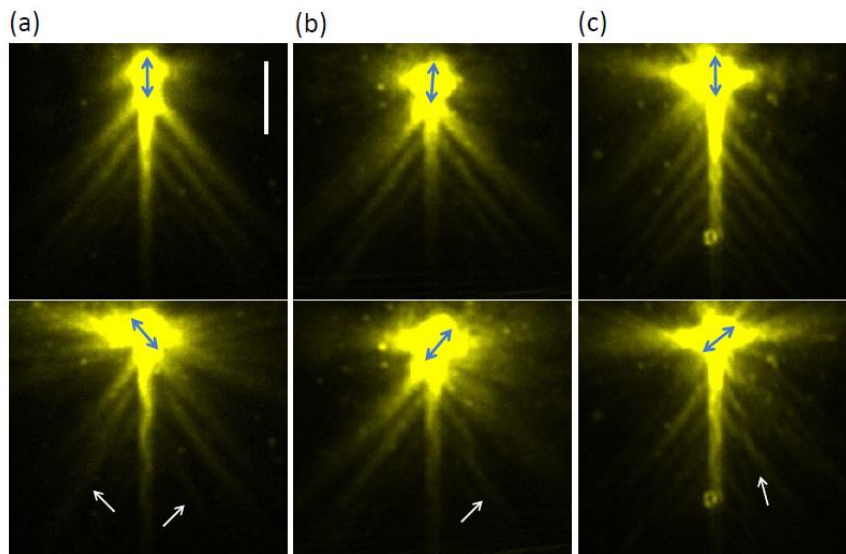


Figure S4. Quantum-dot-fluorescence images for three Ag NW/ Al_2O_3 /Ag film

structures. The spacer thickness is $H = 50$ nm. The blue arrows indicate the polarization of the laser light. The white arrows are guides for eye. The length of the scale bar in (a) is $5 \mu\text{m}$, and applies to all images.

4. The influence of the cross-sectional shape of the NW

The chemically-synthesized Ag NW usually has a pentagonal cross-sectional shape. The pentagonal NW supports similar SPP modes as the cylindrical NW. Figure S5 shows the field distributions and $\text{Re}(k)$ as a function of spacer thickness of the two eigenmodes for a pentagonal NW. As can be seen, the SPP eigenmodes on the NW have very similar field distributions as that shown in Figure 3a. Comparing Figure 3b with Figure S5b shows that the SPP modes on the NW with pentagonal cross section have slightly larger effective refractive index than the modes on cylindrical NW, which is due to the concentration of field at the sharp corners. However, the calculated angles of the collimated SPP beams on the film accord well for the two kinds of NWs as shown in Figure S6. Therefore, the cylindrical NW can be taken as a good model for the realistic NW in this study.

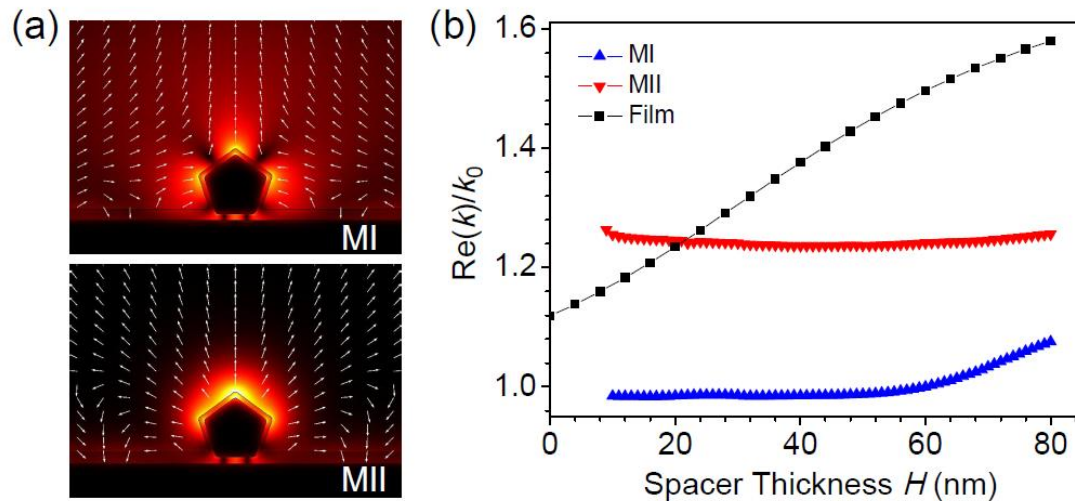


Figure S5. (a) Simulated electric field distributions of the two leaky SPP modes on the Ag NW with pentagonal cross section. The sample parameters in the simulations are $R = 200$ nm (here R refers to the distance between the top left and top right corners of the NW), $H = 40$ nm, $T = 30$ nm, and Ag film thickness 120 nm. The wavelength is 632.8 nm. (b) Simulated real parts of the wave vectors $\text{Re}(k)$ of the two

SPP modes on the NW, as well as the SPPs on the film, as a function of the spacer thickness H . The k_0 is the wave vector of the excitation light. Blue, red and black curves correspond to mode MI, MII and film-SPPs, respectively. The values for R , T , Ag film thickness and wavelength are the same as those in panel a.

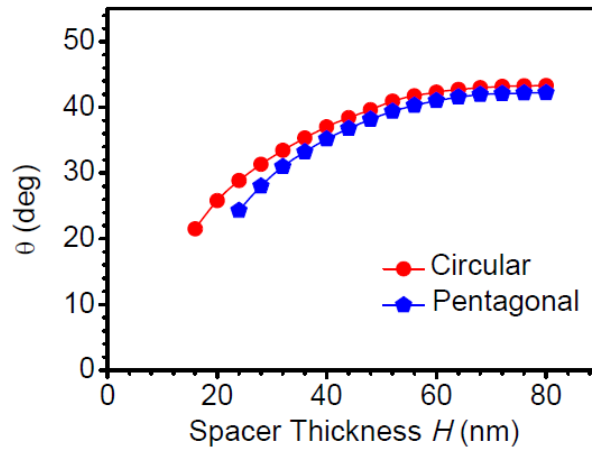


Figure S6. Calculated angles of collimated SPP beams as a function of spacer thickness for Ag NW with circular or pentagonal cross section.

REFERENCES:

- (1) Zhang, S. P.; Wei, H.; Bao, K.; Hakanson, U.; Halas, N. J.; Nordlander, P.; Xu, H. X. *Phys. Rev. Lett.* **2011**, *107*, 096801.
- (2) Wei, H.; Zhang, S. P.; Tian, X. R.; Xu, H. X. *Proc. Natl. Acad. Sci. USA* **2013**, *110*, 4494-4499.